Developmental Cell
Article

Colonization of the Satellite Cell Niche by Skeletal Muscle Progenitor Cells Depends on Notch Signals

Dominique Bröhl,[1] Elena Vasyutina,[1,4] Maciej T. Czajkowski,[1] Joscha Griger,[1] Claudia Rassek,[1] Hans-Peter Rahn,[2] Bettina Purfürst,[3] Hagen Wende,[1] and Carmen Birchmeier[1,*]
[1]Developmental Biology/Signal Transduction Group
[2]Preparative Flow Cytometry Facility
[3]Electron Microscopy Core Facility
Max Delbrück Center for Molecular Medicine, Robert-Rössle-Str. 10, 13125 Berlin, Germany
[4]Present address: Department of Medicine 1, University of Cologne, Kerpener Str. 62, 50924 Cologne, Germany
*Correspondence: cbirch@mdc-berlin.de
http://dx.doi.org/10.1016/j.devcel.2012.07.014

SUMMARY

Skeletal muscle growth and regeneration rely on myogenic progenitor and satellite cells, the stem cells of postnatal muscle. Elimination of Notch signals during mouse development results in premature differentiation of myogenic progenitors and formation of very small muscle groups. Here we show that this drastic effect is rescued by mutation of the muscle differentiation factor *MyoD*. However, rescued myogenic progenitors do not assume a satellite cell position and contribute poorly to myofiber growth. The disrupted homing is due to a deficit in basal lamina assembly around emerging satellite cells and to their impaired adhesion to myofibers. On a molecular level, emerging satellite cells deregulate the expression of basal lamina components and adhesion molecules like integrin α7, collagen XVIIIα1, Megf10, and Mcam. We conclude that Notch signals control homing of satellite cells, stimulating them to contribute to their own microenvironment and to adhere to myofibers.

INTRODUCTION

Stem cells reside in specialized environments, termed stem cell niches, that produce factors that regulate stem cell behavior. Adhesive interactions keep stem cells in their niches close to these factors. In *Drosophila*, cadherins mediate adhesive interactions between male gonadal stem cells and the hub cells in the niche and thereby control the maintenance of stem cells (Song et al., 2002). Integrin-mediated adhesion between ovarial stem cells and the stroma retains follicle stem cells in their niche in the *Drosophila* ovary and has been implicated in the homing of spermatogonial and hematopoietic stem cells, as well as in the maintenance of skin stem cells in mammals (reviewed in Raymond et al., 2009; Marthiens et al., 2010). The stem cells of the muscle (satellite cells) reside between the basal lamina and plasma membrane of myofibers, and we refer to this anatomical position as the stem cell niche. Although they were originally defined by anatomical criteria, recent work indicates that satellite cells receive functionally important cues in their niche (Kuang et al., 2008; Bjornson et al., 2012; Mourikis et al., 2012). The cellular and molecular mechanisms that control the colonization of the niche have not been defined.

Progenitor and stem cells associated with the muscle allow skeletal muscle development, growth, and regeneration. A pool of myogenic progenitor cells is established during development that provides a source of cells for muscle growth in development and generates satellite cells in the perinatal period (Gros et al., 2005; Kassar-Duchossoy et al., 2005; Relaix et al., 2005). These progenitor cells express *Pax7* and *Pax3*, and either self-renew or give rise to differentiating myoblasts. The latter express myogenic determination genes like *MyoD* and *Myf5* that initiate the muscle-specific differentiation program (Rudnicki et al., 1993; Tapscott, 2005). Late in fetal development, a basal lamina forms around muscle fibers (Rosen et al., 1992). In parallel, progenitor cells adopt a satellite cell position, i.e., they locate between the basal lamina and plasma membrane of myofibers. This anatomical position is distinct from the one observed at earlier stages, when progenitors only loosely associate with the fibers (Gros et al., 2005; Kassar-Duchossoy et al., 2005; Relaix et al., 2005). After satellite cells assume their appropriate positions, they initially remain proliferative and generate cells for muscle growth during the perinatal and postnatal periods. This results in a continuous increase in the numbers of nuclei in muscle fibers (White et al., 2010). Satellite cells in mice become quiescent around the time of weaning (postnatal day 21), a process that depends on canonical Notch signals and its target genes Hey1 and Heyl, as well as on Sprouty1, a negative regulator of tyrosine kinase signaling (Shea et al., 2010; Fukada et al., 2011; Bjornson et al., 2012; Mourikis et al., 2012). Upon injury, satellite cells are reactivated to generate myogenic cells for muscle repair and the replenishment of the stem cell pool (Sherwood et al., 2004; Collins et al., 2005).

The signals that maintain the myogenic progenitor/stem cell pool during embryonic, fetal, and postnatal development are under intense investigation. Bone morphogenetic proteins,

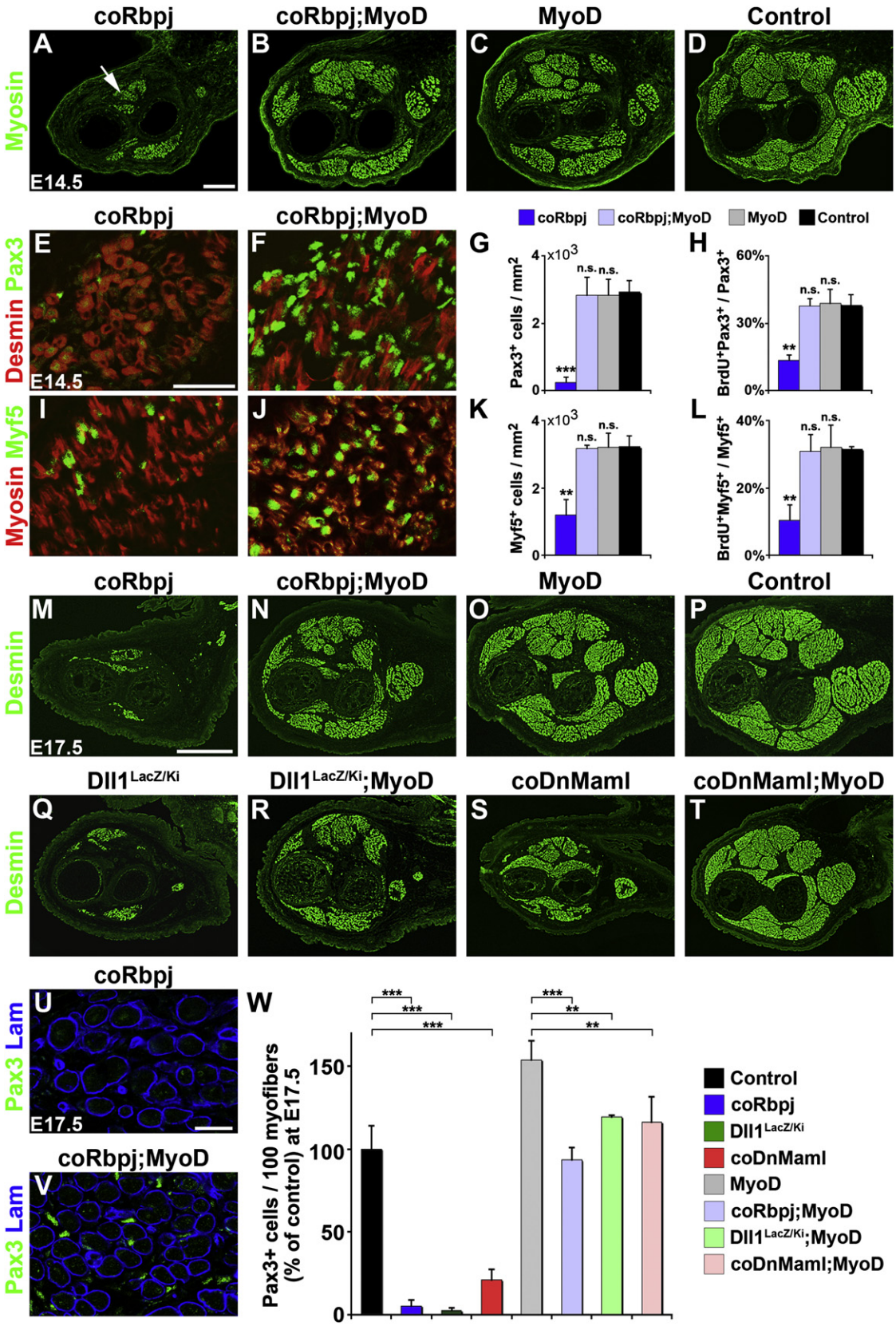
coRbpj
coRbpj;MyoD
MyoD
Control
Myosin
A
B
C
D
E14.5
Desmin Pax3
E
F
Myosin Myf5
I
J
G
H
K
L
coRbpj
coRbpj;MyoD
MyoD
Control
Pax3+ cells / mm2
BrdU+Pax3+ / Pax3+
Myf5+ cells / mm2
BrdU+Myf5+ / Myf5+
n.s.
**
***
Desmin
M
N
O
P
E17.5
DII1LacZ/Ki
DII1LacZ/Ki;MyoD
coDnMaml
coDnMaml;MyoD
Q
R
S
T
Pax3 Lam
U
V
W
Pax3+ cells / 100 myofibers (% of control) at E17.5
Control
coRbpj
DII1LacZ/Ki
coDnMaml
MyoD
coRbpj;MyoD
DII1LacZ/Ki;MyoD
coDnMaml;MyoD

fibroblast growth factors, and canonical and noncanonical Wnt and Notch signals are believed to participate (Kuang et al., 2008; Relaix and Marcelle, 2009; Abou-Khalil and Brack, 2010). Activated Notch signaling has long been known to suppress myogenic differentiation in cultured C2C12 cells, primary satellite cells, and developing chick embryos (Kopan et al., 1994; Shawber et al., 1996; Kuroda et al., 1999; Delfini et al., 2000; Hirsinger et al., 2001; Conboy and Rando, 2002). Recent genetic work showed that mutation of the Notch ligand, *Dll1*, or the transcriptional mediator of Notch signaling, *Rbpj*, results in early depletion of the myogenic progenitor pool due to premature differentiation and the formation of tiny muscle groups that lack myogenic progenitors and satellite cells (Schuster-Gossler et al., 2007; Vasyutina et al., 2007). In contrast, mutation of *Notch3* results in an increase of satellite cells and an overgrowth of muscles upon repeated muscle injury (Kitamoto and Hanaoka, 2010).

Notch signaling in vertebrates and invertebrates is evolutionarily highly conserved and controls growth, differentiation, and patterning (Kimble and Simpson, 1997; Lewis, 1998; Artavanis-Tsakonas et al., 1999). Canonical Notch signaling is initiated by ligand binding (of Dll1, 3 and Jag1, 2 in mice) to the receptors (Notch1-4 in mice), which results in proteolytic cleavage of the intracellular domain of Notch and its transport to the nucleus. This intracellular domain interacts directly with Rbpj (also known as Rbpsuh or CSL), the primary transcriptional mediator of Notch signaling, and with mastermind-like (Maml), which allows the recruitment of the p300 coactivator and the expression of direct Notch target genes like *Hes1*, *Hey1*, and *Heyl* (Jarriault et al., 1995; Wu et al., 2000). Distinct Notch receptors display different functional activities, and notably, the intracellular domain of Notch1 is a potent activator of *Hes1/5* promoters, while the Notch3 intracellular domain is a weaker activator and represses Notch1-mediated *Hes1/5* activation in certain contexts (Beatus et al., 1999).

The bHLH transcription factor MyoD drives myogenic differentiation and cooperates with Myf5 and Mrf4 to control myogenesis in vivo (Rudnicki et al., 1993; Kassar-Duchossoy et al., 2004). Myogenesis proceeds in mice that lack *MyoD*, but muscle differentiation is delayed by ~2 days in paraxial muscles and is accompanied by upregulated expression of *Myf5* (Rudnicki et al., 1992; Kablar et al., 2003). Various molecular mechanisms have been proposed to mediate Notch-dependent suppression of myogenic differentiation, including suppression of *MyoD* (see Buas and Kadesch, 2010 for a recent review). We previously reported that the depletion of the myogenic progenitor pool in *Rbpj* mutant mice is accompanied by rapid MyoD upregulation (Vasyutina et al., 2007). We now show that progenitor depletion is rescued by ablation of *MyoD*. However, rescued myogenic progenitors in *Rbpj;MyoD* double mutants do not assume a satellite cell position. Instead, they locate to the interstitial space of the muscle and contribute poorly to myofiber growth. We provide evidence that Notch signaling controls the assembly of the basal lamina around emerging satellite cells, and promotes the sustained adhesion between satellite cells and myofibers.

RESULTS

Mutation of MyoD Rescues the Myogenic Stem Cell Pool in Notch Signaling Mutants

Conditional mutation of *Rbpj* in myogenic progenitors (*Pax3^{cre}; Rbpj$^{flox/flox}$*; referred to as *coRbpj*) led to premature differentiation of the progenitor cells, resulting in the formation of tiny muscle groups (shown at E14.5 in Figure 1A; the control is displayed in Figure 1D; cf. Vasyutina et al., 2007). We examined whether MyoD upregulation might be involved and analyzed muscle from *coRbpj;MyoD* double mutants. At E14.5, a pronounced rescue of muscle development was observed, with the overall muscle mass in *coRbpj;MyoD* and *MyoD* single mutants being virtually indistinguishable (Figures 1B and 1C). Indeed, comparable numbers of Pax3+ or Myf5+ cells were associated with the muscles of control, *coRbpj;MyoD$^{-/-}$*, and *MyoD$^{-/-}$* mice, and these cells displayed similar proliferative capacities at E14.5 (Figures 1E, 1F, 1I, and 1J; quantified in Figures 1G, 1H, 1K, and 1L). The pronounced rescue was observable in limb and back muscles but not in diaphragm muscles (Figures 1A–1D; Figures S1A, S1B, S1J, and S1K available online). The absence of the diaphragm muscle may be a cause of the postnatal lethality of *coRbpj;MyoD$^{-/-}$* mice. We conclude that Rbpj maintains the myogenic progenitor pool by suppressing MyoD.

Further analysis indicated, however, that mutation of *MyoD* did not completely rescue late fetal muscle development of *coRbpj* mutants. For example, although the muscle mass of *coRbpj;MyoD$^{-/-}$* mice increased after E14.5, at E17.5 it had not reached the mass observed in *MyoD$^{-/-}$* mice (Figures 1M and 1N; for comparison, see *MyoD$^{-/-}$* and control muscles in Figures 1O and 1P; for a quantification, see below). We also compared a strong hypomorph *Dll1* mutation that results in a muscle phenotype similar to that seen in *coRbpj* mutants

Figure 1. *MyoD*-Dependent Rescue of the Myogenic Progenitor Pool in Mice with Disrupted Notch Signaling

(A–D) Immunohistological analyses of limb muscle at E14.5 in *coRbpj*, *coRbpj;MyoD$^{-/-}$*, *MyoD$^{-/-}$*, and control mice. The muscle was visualized in animals with the indicated genotypes using antibodies against skeletal muscle-specific myosin.

(E–L) Analysis of Pax3+ (E and F) and Myf5+ (I and J) cells associated with back muscle of E14.5 *coRbpj* (E and I) and *coRbpj;MyoD$^{-/-}$* (F and J) mice by immunohistology. The arrow in (A) points to the tiny muscle formed in *coRbpj* mice. (G and K) Quantification of the numbers of Pax3+ and Myf5+ cells per mm^2 and (H and L) their proliferation capacity (proportion of BrdU+Pax3+ cells/Pax3+ cells and BrdU+Myf5+ cells/Myf5+ cells) in mice with the indicated genotypes.

(M–T) Immunohistological analyses of limb muscle in mice with disrupted Notch signaling (i.e., *Dll1$^{LacZ/Ki}$*, *coDnMaml* and the corresponding *MyoD* double mutants), using antibodies against desmin at E17.5. The genotypes of the animals are indicated.

(U and V) The myogenic progenitor pool in back muscle was analyzed in E17.5 *coRbpj* and *coRbpj;MyoD$^{-/-}$* mice by costaining with antibodies directed against Pax3 and laminin.

(W) Quantification of the numbers of Pax3+ cells at E17.5 per 100 myofibers of the indicated genotypes compared with the one in control that was set as 100%. Error bars, SD. Statistical significance is indicated [compared with control mice in (G), (H), (K), and (L)]; **p < 0.01; ***p < 0.001; n.s., not significant). Scale bars: 200 μm in (A), 30 μm in (E), 500 μm in (M), and 20 μm in (U).

See also Figure S1.

(Schuster-Gossler et al., 2007), and again observed a pronounced but not complete rescue of limb and back muscle mass in *Dll1*$^{LacZ/Ki}$*;MyoD* compound mutants at E17.5 (Figures 1Q, 1R, S1E, and S1F; see quantification below). Dominant-negative Maml (DnMaml) interferes with Notch signaling by forming an inactive Rbpj complex. *Pax3*^{cre}-induced expression of *DnMaml* from the *ROSA26* locus (called the *coDnMaml* mutant; cf. Tu et al., 2005) also resulted in a reduction of the muscle mass, which was less pronounced than that of *coRbpj* or *Dll1*$^{LacZ/Ki}$ mice at E17.5 (Figure 1S). This indicates that the transgenic expression of *DnMaml* downregulates but does not eliminate canonical Notch signaling. Despite the milder effects of the *coDnMaml* mutation, mutation of *MyoD* did not completely rescue the muscle mass of *coDnMaml* mice at E17.5 (Figures 1T, S1G, and S1H; see quantification below). This provided a first indication that suppression of MyoD is an important but not the sole readout of Notch signaling during muscle development.

Progenitor cells associated with the muscle tissue in the various mutants at E17.5 were analyzed and quantified (Figures 1U–1W). In control mice, we observed 33.4 ± 5.6 Pax3+ cells/100 myofibers, which was set as 100% (Figure 1W). Pax3+ cells were rare in *coRbpj* or *Dll1*$^{LacZ/Ki}$ mutants, and their numbers were strongly reduced in *coDnMaml* mutants (Figure 1W). When the *MyoD* mutation was introduced into the *coRbpj*, *Dll1*$^{LacZ/Ki}$, and *coDnMaml* mutant backgrounds, the numbers of Pax3+ cells increased dramatically and reached 93.4%, 119.4%, and 116.2% of those observed in control mice (Figure 1W). It should be noted that the muscle of *MyoD* mutants contained 153.8% progenitor cells compared with control mice (cf. Seale et al., 2004), and that the progenitor cell numbers in all three double mutants did not reach such levels (Figure 1W). The proliferative activity of the Pax3+ cells in the double-mutant mice was only mildly affected (Figure S1I). We conclude that during late fetal stages, the *MyoD* mutation rescues muscle development substantially but not completely.

Notch Signals Are Required for Satellite Cell Homing

Satellite cells represent the stem cells of the adult muscle. They are wedged between the basal lamina and plasma membrane of myofibers (Mauro, 1961) and emerge around E15.5, when a basal lamina forms around myofibers (Gros et al., 2005; Kassar-Duchossoy et al., 2005; Relaix et al., 2005; see Figure 2A for a scheme displaying the anatomical position of satellite cells). We therefore sought to determine whether satellite cells formed correctly in the various single and double mutants, and quantified the numbers of Pax3+ cells (number of cells/100 fibers) that were located below the basal lamina (Figures 2B–2F; arrows point toward satellite cells; quantified in Figure 2G). Remarkably, few Pax3+ cells settled correctly in *coRbpj;MyoD*$^{-/-}$, *Dll1*$^{LacZ/Ki}$*;MyoD*$^{-/-}$, and *coDnMaml;MyoD*$^{-/-}$ animals. Instead, the vast majority of Pax3+ cells located in the interstitial space of the muscle in the double mutants (Figures 2B–2D; arrowheads point toward the unusual interstitial Pax3+ cells; quantified in Figure 2H). It should be noted that *MyoD* mutants display a 1.5-fold increase in the number of Pax3+ cells compared with control mice, but the number of Pax3+ cells below the basal lamina remained constant and the supernumerary cells located to the interstitial space. Thus, 28.5% of all Pax3+ cells in control mice located to the interstitial space, whereas 49.9% and 92.3% located interstitially in *MyoD*$^{-/-}$ and *coRbpj;MyoD*$^{-/-}$ animals, respectively (Figure 2F; Pax3+ cells in the interstitial space are quantified in Figure 2H). The heterozygous *MyoD* mutation affected neither satellite cell number nor homing (Figure S2). Electron microscopy confirmed the disrupted emergence of satellite cells in *coRbpj;MyoD*$^{-/-}$ mice, and in control mice these were clearly seen as myofiber-associated cells below the basal lamina (Figures 2I and 2J; quantified in Figure 2K; arrowheads point toward the basal lamina surrounding myofiber and satellite cell in control mice). Thus, despite the substantial rescue of the progenitor pool in double mutants, colonization of the satellite cell niche was severely disrupted in the muscle of *Notch/MyoD* double mutants. In *MyoD* mutant mice, interstitial cells were more abundant, but the number of cells that assumed a satellite cell position was unchanged, indicating that the major deficit in homing observed in *coRbpj;MyoD*$^{-/-}$ mice can be assigned to the *Rbpj* mutation. It is interesting to note that Pax3+ cells in the interstitial space were not surrounded by a continuous basal lamina (Figures 2B–2E).

We next tested the proliferation or survival of Pax3+ cells that settled between the basal lamina and plasma membrane of myofibers or outside in the interstitial space. Pax3+ cells in *coRbpj;MyoD* mutants displayed a small reduction in proliferation compared with those present in *MyoD* mutants or control animals, regardless of where they settled (Figures 2L–2N). We assessed apoptosis by analyzing cleaved caspase 3 (E17.5). In general, apoptosis rates were small. We observed a trend toward increased cell death of interstitial Pax3+ cells in *coRbpj;MyoD* double mutants (0.000, 0.001, and 0.006 cleaved caspase 3+ Pax3+ cells/total Pax3+ cells in control, *MyoD*$^{-/-}$, and *coRbpj;MyoD*$^{-/-}$ mice, respectively), but this difference was not statistically significant. Thus, neither decreased proliferation nor preferential loss of cells by apoptosis can account for the disrupted homing of emerging satellite cells in the *coRbpj;MyoD*$^{-/-}$ muscle. We conclude that progenitor cells require Notch signals to settle in a satellite cell position.

We next asked whether mislocated progenitor cells contribute correctly to myofiber growth in *coRbpj;MyoD* mutants. Nuclei in myofibers were counted, and their numbers differed little between *MyoD* and *coRbpj;MyoD* mutant mice up to E15.5. However, the subsequent fiber growth was severely blunted in *coRbpj;MyoD*$^{-/-}$ mice, and compared with *MyoD* mutants, we observed a 54% reduction in the number of myonuclei/myofibers 4 days later (Figures 3A–3E). This provides further evidence that Notch signals serve additional important functions in late fetal myogenesis that go beyond *MyoD* suppression. We also tested whether disrupted secondary myogenesis, which occurs in the late fetal period and generates fast myofibers, accounts for this. Fast and slow myofibers were present in similar proportions, and secondary myofibers had formed under the same basal lamina as primary fibers in the muscle of *MyoD* and *coRbpj;MyoD* mutant mice (Figures S3A–S3D). The in vitro fusion capacities of progenitor cells obtained from *coRbpj;MyoD*$^{-/-}$ and *MyoD*$^{-/-}$ mice at E17.5 were comparable (Figures 3F–3I). Thus, the disrupted myofiber growth is not due to disrupted secondary myogenesis or to altered fusion capacity.

Pax7 and the paralogous Pax3 protein are coexpressed in myogenic progenitor cells in trunk muscle of control and *MyoD*$^{-/-}$ mice at E17.5 (Figure 3J). Remarkably, the Pax3+ cells

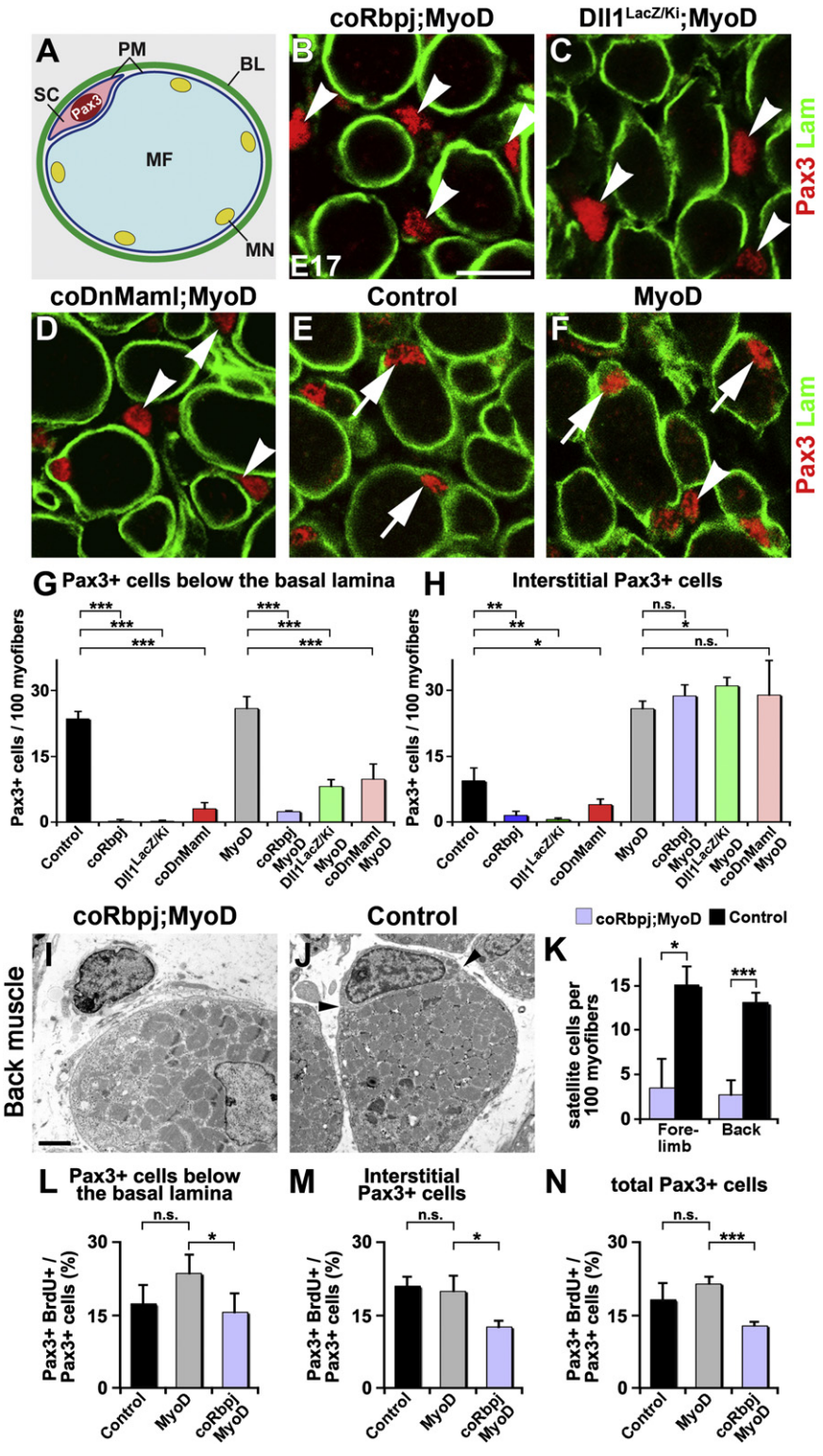

Figure 2. Canonical Notch Signaling Is Required for Satellite Cell Homing

(A) Schematic diagram showing the anatomical localization of satellite cells (SC) wedged between the basal lamina (BL) and the myofiber (MF) plasma membrane (PM). Myonuclei (MN) are shown in yellow.

(B–F) Analysis of emerging satellite cells at E17.5 using antibodies against Pax3 (red) and laminin (green). Shown are sections of back muscle from mice with the indicated genotypes. Arrowheads point toward Pax3+ cells located in the interstitial space, which are abundant in the *MyoD/Notch* signaling double mutants.

(G and H) Quantification of Pax3+ cells located below the basal lamina of muscle fibers (G) and in the interstitial space (H).

(I–K) Analysis of emerging satellite cells in *coRbpj;MyoD*$^{-/-}$ (I) and control (J) E17.5 mice using electron microscopy, and their quantification (K) in forelimb and back muscle. The arrowheads in (J) point toward the contact site between a myofiber and satellite cell located below a basal lamina in control mice.

(L–N) Proliferation of Pax3+ cells in control, *MyoD*$^{-/-}$, and *coRbpj;MyoD*$^{-/-}$ mice. The proliferation of cells located below the myofiber basal lamina or in the interstitial space, as well as the proliferation of all Pax3+ cells, were assessed. Error bars, SD. Statistical significance is indicated (*$p < 0.05$; **$p < 0.01$; ***$p < 0.001$; n.s., not significant). Scale bar: 15 μm in (B) and 2 μm in (I). See also Figure S2.

did not coexpress Pax7 in *coRbpj;MyoD* and *Dll1*$^{LacZ/Ki}$*;MyoD* double-mutant muscle, and *Pax7* mRNA was downregulated in a pronounced manner, as assessed by quantitative real-time PCR (qRT-PCR; Figures 3J and 3K). Downregulated Pax7 protein in *coRbpj;MyoD* mutant muscle was also noted at E14.5 and E11.5 (data not shown). In contrast, in *coDnMaml;MyoD*$^{-/-}$ mice, the Pax3+ cells coexpressed Pax7 protein, whereas qRT-PCR indicated a mild downregulation of the corresponding mRNA (Figures 3J and 3K). It should be noted that Pax3+ cells coexpressed Myf5 but not markers of endothelial (Pecam) or smooth muscle cells (smooth muscle actin) in *coRbpj;MyoD*$^{-/-}$ mice (Figures S3E–S3J). We conclude that correct Pax7 expression in myogenic progenitors depends on Notch signaling.

Disrupted Cell Adhesion and Basal Lamina Assembly of Emerging Satellite Cells in Notch Signaling Mutants

We next examined which mechanism might be responsible for the disrupted homing of satellite cells. Emerging satellite cells and myofibers interact, and proteins produced by fibers or progenitor cells may be required for homing. Immunohistochemical analysis showed that Rbpj is strongly expressed in Pax3+ and MyoD+ cells of wild-type muscle (Figures 4A, 4A′, 4A″, 4B, and 4B′; arrows point toward Pax3+ and MyoD+ cells coexpressing Rbpj), but little or no

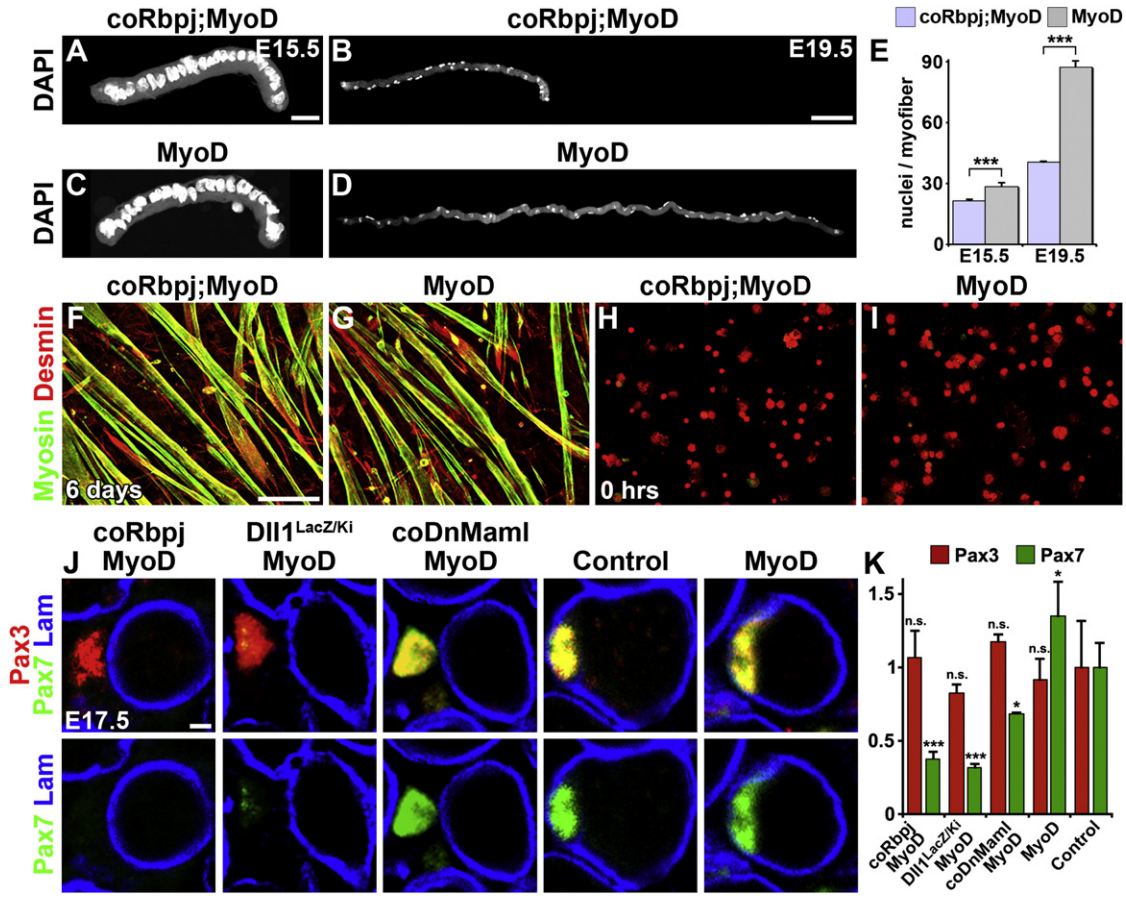

Figure 3. The *MyoD* Mutation Does Not Rescue Notch Signaling-Dependent Fiber Growth and Pax7 Expression

(A–D) Isolated myofibers obtained from *coRbpj;MyoD*$^{-/-}$ and *MyoD*$^{-/-}$ mice at E15.5 (A and C) and E19.5 (B and D) stained with DAPI.

(E) Quantification of nuclei/myofiber isolated from *coRbpj;MyoD*$^{-/-}$ and *MyoD*$^{-/-}$ mice.

(F–I) Culture of isolated cells from *coRbpj;MyoD*$^{-/-}$ and *MyoD*$^{-/-}$ mice after 6 days in differentiation medium (F and G) and directly after plating (H and I).

(J) Analysis of Pax7 and Pax3 coexpression by immunohistology of back muscle of *coRbpj;MyoD*$^{-/-}$, *Dll1*$^{LacZ/Ki}$*;MyoD*$^{-/-}$, *coDnMaml;MyoD*$^{-/-}$, control, and *MyoD*$^{-/-}$ mice at E17.5. The upper and lower panels show the same sections stained with antibodies against Pax7, Pax3, and laminin. The upper panels display Pax3/Pax7/laminin, and the lower panels show Pax7 and laminin signals.

(K) Quantification of *Pax7* and *Pax3* mRNA isolated from back muscle tissue by qRT-PCR. Error bars, SD. Statistical significance is indicated [compared with control mice in (K); *p < 0.05; ***p < 0.001; n.s., not significant]. Scale bars: 20 μm in (A), 100 μm in (B) and (F), and 2 μm in (J).

See also Figure S3.

Rbpj or MyoD was detectable in the myofibers (arrowheads in Figures 4A–4A″). More than 90% of all Pax3+ cells coexpressed Rbpj, and approximately one-third were triple-positive for Rbpj, Pax3, and MyoD. Rbpj was not detectable in Pax3+ cells of *coRbpj;MyoD* mutants, demonstrating the specificity of the antibody (Figure 4C). Thus, Rbpj is transiently expressed and quickly downregulated in differentiated fibers. We therefore concentrated our further analyses on emerging satellite cells and defined their expression profiles to identify genes responsible for the disrupted homing.

We isolated myogenic progenitor cells from fetal mice at E17.5 by fluorescence-activated cell sorting (FACS), using a modification of a previously established protocol (see Experimental Procedures; Kuang et al., 2007), and verified the identity of the sorted cells by analyzing Pax7 and/or Pax3 expression (Figures 4G–4I). At the stage when satellite cells emerge, the muscles of *coRbpj*, *Dll1*$^{LacZ/Ki}$, or *coDnMaml* mutants contain few progenitor cells, and the low abundance did not allow us to isolate a pure population of these cells. We therefore sorted cells (Vcam-1+/CD31−/CD45−/Sca1− cells) from wild-type, *MyoD*$^{-/-}$, *coRbpj;MyoD*$^{-/-}$, and *coDnMaml;MyoD*$^{-/-}$ mice, and used these cells for RNA isolation and microarray analysis. We identified differentially expressed genes using a Bonferroni-corrected p-value of <0.0001 as a cutoff (Figure 4J). We defined genes consistently deregulated in *coRbpj;MyoD*$^{-/-}$ and *coDnMaml;MyoD*$^{-/-}$ cells, i.e., 88 downregulated genes in cluster 1, and 108 upregulated genes in clusters 2 and 3 (see Table S1 for a list of all deregulated genes). Among the downregulated genes in cluster 1 (Figure 4J; cluster 1 is also shown in Table 1) were Notch receptors (*Notch1* and *3*) and direct Notch target genes like *Hey1*, *Heyl*, *Dtx4*, and *Msc* (Buas et al., 2009). Notch target genes were downregulated in a pronounced manner in *coRbpj;MyoD*$^{-/-}$ and *coDnMaml;MyoD*$^{-/-}$ cells. Notch receptors and targets were also mildly downregulated in the isolated cells from *MyoD* mutants. Thus,

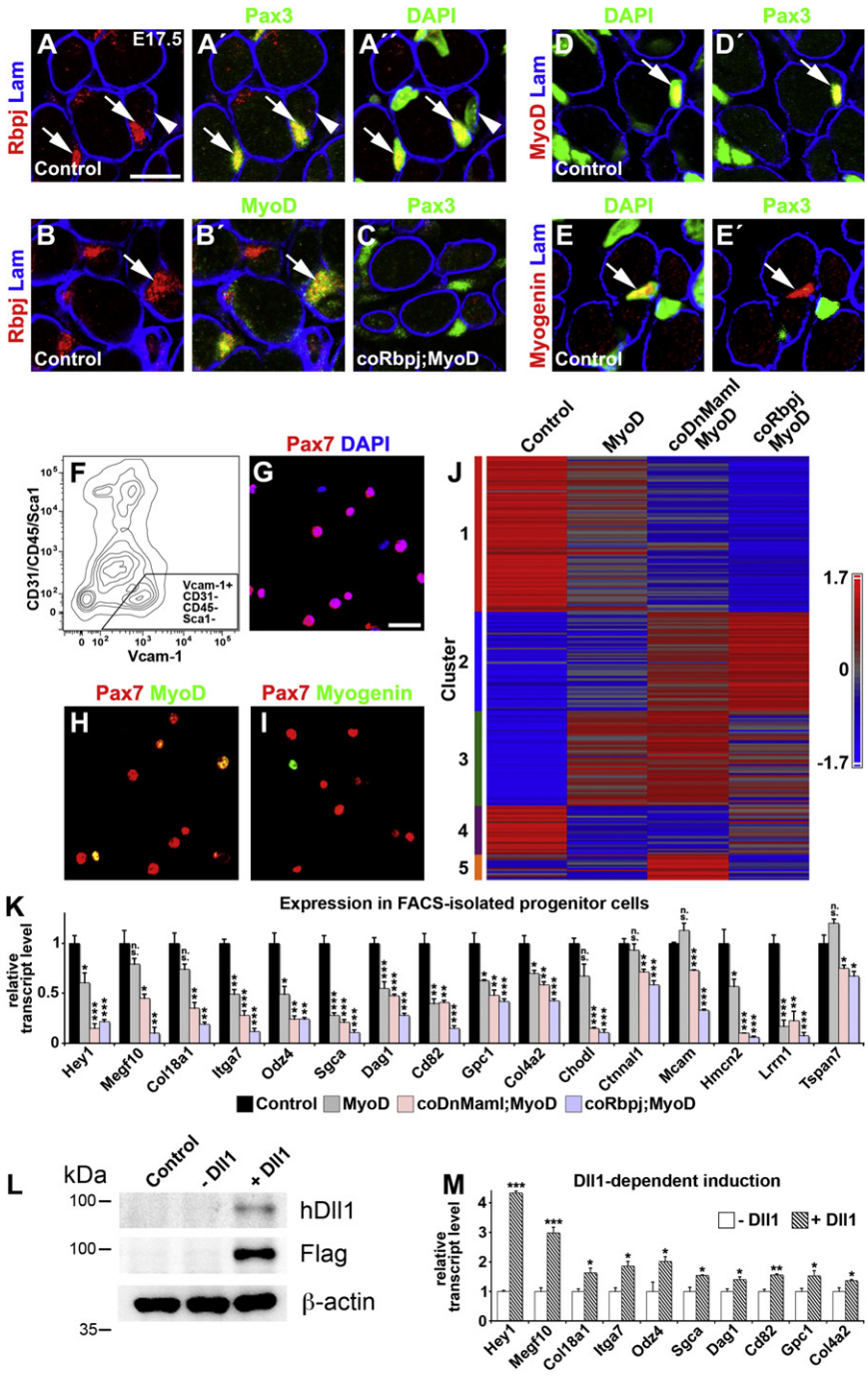

Figure 4. Molecular Characterization of Myogenic Progenitor Cells in Notch Signaling Mutants

(A–A″) Immunohistological analysis of control muscle at E17.5 using antibodies directed against Rbpj, laminin, and Pax3; the section was also counterstained with DAPI. Note that (A), (A′), and (A″) show the same section and display Rbpj/laminin, Rbpj/Pax3/laminin, and Rbpj/DAPI/laminin signals, respectively. Nuclei of myogenic progenitors (arrows) were defined by DAPI staining and the presence of Pax3 and/or MyoD or myogenin. Myofiber nuclei (arrowheads) were defined by DAPI staining, their location inside the laminin+ matrix, and the absence of Pax3 and MyoD signals.

(B and B′) Immunohistological analysis of Rbpj, laminin, and MyoD in control muscle. Note that B and B′ show the same section and display Rbpj/laminin and Rbpj/MyoD/laminin signals, respectively.

(C) Immunohistological analysis of muscle from *coRbpj;MyoD*$^{-/-}$ mice using antibodies against Rbpj, Pax3, and laminin.

(D and D′) Immunohistological analysis of MyoD, laminin, and Pax3 in control muscle; the section was also counterstained with DAPI. Note that (D) and (D′) show the same section and display MyoD/laminin/DAPI and MyoD/laminin/Pax3 signals, respectively.

(E and E′) Immunohistological analysis of myogenin, laminin, and Pax3 in control muscle; the section was also counterstained with DAPI. Note that (E) and (E′) show the same section and display myogenin/laminin/DAPI and myogenin/laminin/Pax3 signals, respectively.

(F) FACS analysis of muscle cells using antibodies directed against Vcam-1, CD31, CD45, and Sca1. The gate used to isolate cells is indicated.

(G–I) Immunohistological analysis of sorted and directly cytospun cells using Pax7, MyoD, and myogenin antibodies; the cells were counterstained by DAPI.

(J) Heat map of deregulated genes identified by microarray experiments of FACS-isolated cells obtained from control (wild-type), *MyoD*$^{-/-}$, *coDnMaml;MyoD*$^{-/-}$, and *coRbpj;MyoD*$^{-/-}$ mice.

(K) Verification of the deregulated expression of selected genes from cluster 1 by qRT-PCR.

(L) Western blot analysis of untransfected (control), pMX-IRES2-DsRed2- (-Dll1), and pMX-hDll1-IRES2-DsRed2-transfected (+Dll1) 70Z/3 cells. Protein extracts were incubated with antibodies against hDll1, Flag-tag, or β-actin.

(M) Expression of Hey1 and of genes in cluster 1 that encode basal lamina and adhesion molecules was analyzed by qRT-PCR in isolated satellite cells after coculture with transfected 70Z/3 cells expressing Dll1/DsRed (+Dll1) or DsRed only (−Dll1). Only those genes that respond to Dll1 are shown. Error bars, SEM. Statistical significance is indicated (*$p < 0.05$; **$p < 0.01$; ***$p < 0.001$; n.s., not significant). Scale bars: 10 μm in (A) and 25 μm in (G).

See also Figure S4.

loss of *MyoD* may modulate Notch signaling in certain cells, such as the subpopulation of Pax3+ cells that coexpress MyoD in normal development. Our initial immunohistological analyses indicated that basal lamina assembly around emerging satellite cells, but not around myofibers, was severely disrupted in *coRbpj;MyoD* mutants (see below). Interestingly, 17% of the genes in cluster 1 (e.g., *Itga7*, *Col18a1*, *Megf10*, and *Mcam*; Table 1) were previously implicated in basal lamina formation or assembly and cell adhesion. Expression of the majority changed in a more pronounced manner in *coRbpj;MyoD*$^{-/-}$ and *coDnMaml;MyoD*$^{-/-}$ cells than in *MyoD*$^{-/-}$ cells. The deregulated expression of the genes encoding cell adhesion and

Table 1. Genes from Cluster 1 of Microarray Analyses Associated with Basal Lamina Assembly, Cell Adhesion, and Notch Signaling

Category	Symbol	Definition	Fold Change[a] RM	DM	M
Basal lamina assembly	***Col18a1***	***collagen, type XVIII, alpha 1***	***−1,8***	***−1,6***	***−1,2***
	Itga7	***integrin alpha 7***	***−4,5***	***−3,0***	***−1,7***
	Sgca	***sarcoglycan, alpha (dystrophin-associated glycoprotein)***	***−6,9***	***−4,1***	***−3,1***
	Dag1	***dystroglycan 1***	***−2,6***	***−2,5***	***−2,1***
	Cd82	***CD82 antigen***	***−2,8***	***−1,6***	***−1,9***
	Col4a2	*collagen, type IV, alpha 2*	*−1,9*	*−2,0*	*−1,4*
	Chodl	*chondrolectin*	*−6,4*	*−4,1*	*−1,7*
	Hmcn2	*hemicentin 2*	*−13,0*	*−9,4*	*−3,4*
	Lrrn1	*leucine rich repeat protein 1, neuronal*	*−3,7*	*−1,5*	*−2,4*
Cell adhesion	***Megf10***	***multiple EGF-like-domains 10***	***−3,1***	***−2,3***	***−1,8***
	Odz4	***odd Oz/ten-m homolog 4 (Drosophila)***	***−3,5***	***−3,3***	***−2,0***
	Gpc1	***glypican 1***	***−1,7***	***−1,4***	***−1,3***
	Ctnnal1	*catenin (cadherin associated protein), alpha-like 1*	*−2,1*	*−1,7*	*−1,3*
	Mcam	*melanoma cell adhesion molecule*	*−1,9*	*−1,2*	*1,1*
	Tspan7	*tetraspanin 7*	*−2,1*	*−1,2*	*1,1*
Notch signaling/targets	***Hey1***	***hairy/enhancer-of-split related with YRPW motif 1***	***−4,7***	***−4,5***	***−2,2***
	Heyl	hairy/enhancer-of-split related with YRPW motif-like	−9,9	−7,3	−3,2
	Dtx4	deltex 4 homolog (Drosophila)	−2,6	−2,4	−1,4
	Msc	musculin	−1,8	−1,6	1,0
	Notch1	Notch gene homolog 1 (Drosophila)	−2,2	−2,5	−1,8
	Notch3	Notch gene homolog 3 (Drosophila)	−5,8	−7,7	−2,8

[a]Fold changes of genes in cluster 1 for the genotypes *coRbpj;MyoD*$^{-/-}$ (RM), *coDnMaml;MyoD*$^{-/-}$ (DM), and *MyoD*$^{-/-}$ (M) compared with control mice. Genes indicated in italics were tested for a response to Dll1 in satellite cells. Genes indicated in bold were induced by the presence of Dll1, indicating that they are direct targets of Notch signaling. See also Table S1.

basal lamina molecules was verified by qRT-PCR (Figure 4K). No major changes in gene expression were detected when sorted progenitor cells of heterozygous *MyoD* mutants and wild-type mice were compared (Figure S4). We also examined whether the identified genes are directly regulated by Notch signaling. For this, satellite cells from wild-type mice were isolated and exposed to a Dll1-expressing 70Z/3 pre-B lymphoblast cell line. This line was generated by transfection of a Dll1-expression vector (pMX-hDll1-IRES2-DsRed2), and cells transfected with a plasmid without Dll1 sequences served as control (pMX-IRES2-DsRed2; Figure 4L). Satellite cells were cocultured for 3 hr in the presence of Dll1+ and Dll1- cells, and the protein translation inhibitor cycloheximide was added to exclude indirect effects on gene expression. Analysis by qRT-PCR demonstrated that many of the identified genes encoding cell adhesion and basal lamina components, for instance *Itga7*, *Col18a1*, *Odz4*, and *Megf10*, responded to Dll1 (Figure 4M). These data demonstrate that Notch signaling directly modulates cell adhesion and basal lamina formation in satellite cells.

We also analyzed the assembly of the basal lamina and adhesion during the time period of satellite cell homing. Collagen XVIIIα1 is a component of basal lamina that possesses structural properties common to both collagens and proteoglycans (Marneros and Olsen, 2005). In control muscle, the collagen-XVIIIα1-containing basal lamina surrounding myofibers is still discontinuous at E14.5 and is not yet directly associated with Pax3+ cells. At E15.5, a weak collagen XVIIIα1 staining is discernible around emerging satellite cells, and by E17.5 a contiguous collagen-XVIIIα1-containing basal lamina surrounds fibers and satellite cells (Figures 5A and 5A′; arrowheads point to emerging basal lamina). Assembly of a collagen-XVIIIα1-containing basal lamina around Pax3+ cells was also observable at E15.5 and E17.5 in *MyoD*$^{-/-}$ muscle (Figures 5B and 5B′). Collagen XVIIIα1 staining associated with Pax3+ cells of *coRbpj;MyoD*$^{-/-}$ mice was consistently very low at all stages analyzed, indicating that these cells do not assemble a collagen-XVIIIα1-containing basal lamina (Figures 5C and C′). In addition to collagen XVIIIα1, laminin also was not assembled around Pax3+ cells in *coRbpj;MyoD*$^{-/-}$ muscle at E17.5, pointing toward a general deficit in the assembly of the basal lamina around emerging satellite cells. Similar changes in basal lamina assembly around emerging satellite cells were present in *coDnMaml;MyoD* mutants (Figures S5A–S5F). It should be noted that only basal lamina assembly around emerging satellite cells, and not around myofibers, was disrupted in *coRbpj;MyoD* and *coDnMaml;MyoD* mutants (Figures 5D–5F and S5G–S5J). *Col18a1* and *Itga7* encode collagen XVIIIα1 and integrin α7, respectively, and integrin α7 is a component of the principal laminin receptor of satellite cells with essential functions in postnatal muscle (Mayer et al., 1997). Both genes were downregulated in the microarray experiments (see Table 1). Our data thus indicate that canonical Notch signals are required for the assembly of the basal lamina surrounding emerging satellite cells.

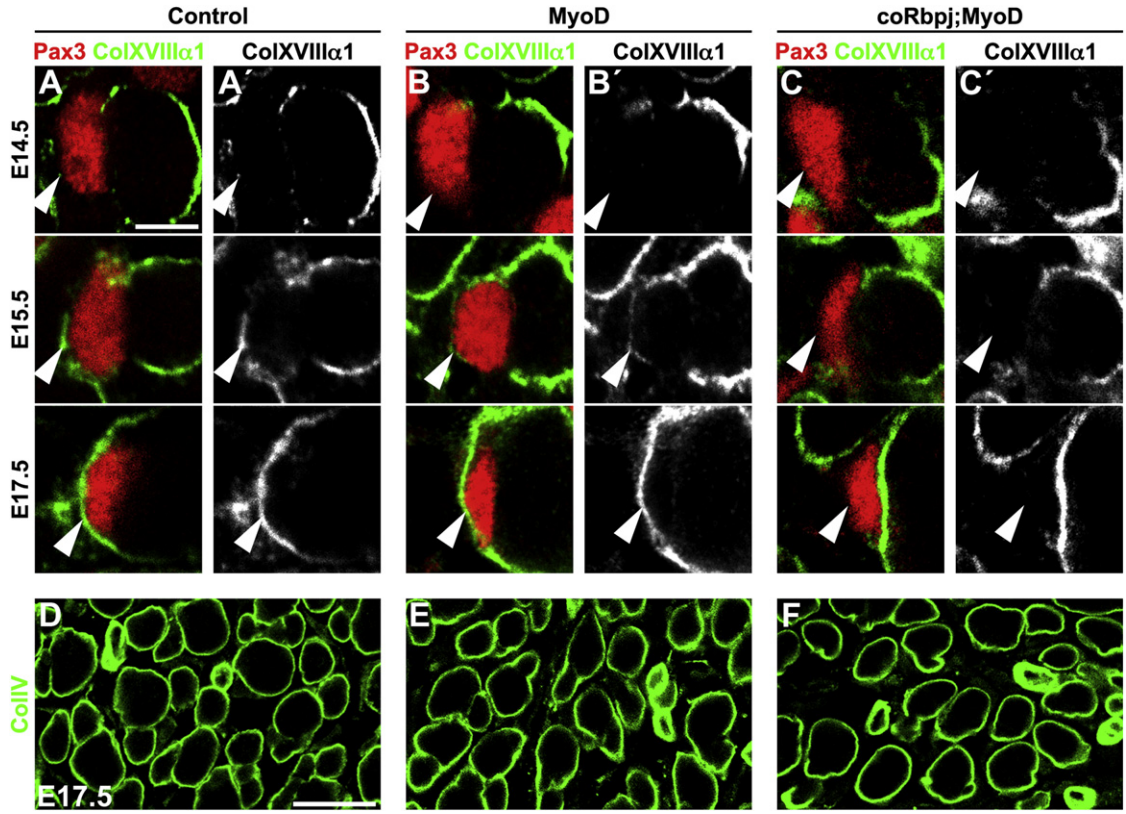

Figure 5. Notch Signals Control Assembly of the Basal Lamina around Emerging Satellite Cells

(A–C′) Collagen XVIIIα1 assembly around Pax3+ cells in muscle of control (A and A′), *MyoD*$^{-/-}$ (B and B′), and *coRbpj;MyoD*$^{-/-}$ (C and C′) mice at indicated stages (E14.5–E17.5). (A) and (A′), (B) and (B′), and (C) and (C′) show the same fibers but display collagen XVIIIα1/Pax3 and collagen XVIIIα1 signals, respectively. (D–F) Immunohistological analysis of collagen IV expression in the back muscle of E17.5 control (D), *MyoD* (E), and *coRbpj;MyoD* (F) mutant mice. Scale bars: 5 μm in (A) and 20 μm in (D). See also Figure S5.

We next defined the adhesion molecules that mediate the attachment of emerging satellite cells to myofibers between E14.5 and E17.5 in control mice. This revealed that M-cadherin, cadherin-associated β-catenin, and talin, a molecule that is recruited to activated integrins (Moser et al., 2009), located to contact sites between emerging satellite cells and myofibers (Figures 6A, 6B, and 6H; arrowheads point to contact sites). Megf10, a transmembrane protein that is implicated in adhesion, engulfment, and myogenic development (Holterman et al., 2007; Suzuki and Nakayama, 2007a, 2007b; Logan et al., 2011), and the adhesion molecule Mcam (Ouhtit et al., 2009) both accumulated at these sites (Figures 6M and 6N; arrowheads point to contact sites). M-cadherin, Vcam-1, talin, Mcam, and Megf10 molecules were also present at adhesive contacts in *MyoD*$^{-/-}$ muscle at E17.5 (arrowheads in Figures 6C, 6D, 6I, 6J, 6O, and 6P).

In *coRbpj;MyoD* mutants, M-cadherin, β-catenin, and talin were present at the contact sites that began to form at E15.5 (Figure 6E; arrowheads point to contact sites; data not shown). However, the contacts were transient and the vast majority of Pax3+ cells had detached in *coRbpj;MyoD*$^{-/-}$ muscle by E17.5 (Figures 6F, 6K, and 6L). Further, low levels of Mcam and Megf10 protein were observable in the plasma membrane of Pax3+ cell at E15.5 and E17.5 (Figures 6Q and 6R; data not shown). *Mcam* and *Megf10* were among the deregulated genes identified in the microarray experiments (see Table 1). Similar transient contacts were observed in *coDnMaml;MyoD* mutant muscle (Figure S6). Our data thus indicate that canonical Notch signals are required for sustained and stable adhesion to myofibers.

DISCUSSION

Satellite cells were originally defined as cells "wedged" between the basal lamina and plasma membrane of myofibers (Mauro, 1961), and this particular anatomical position has been referred to as the satellite cell niche. We show that canonical Notch signaling in emerging satellite cells stimulates these cells to adhere to myofibers and to produce components of the basal lamina that will eventually surround the muscle fiber and the satellite cell.

Notch Signaling, MyoD, and Myogenic Stem Cell Maintenance

Suppression of myogenic differentiation is a well studied function of Notch and has been observed in C2C12 cells, primary satellite cells in culture, developing chicks, and the muscle of the developing and adult mouse (Kopan et al., 1994; Shawber

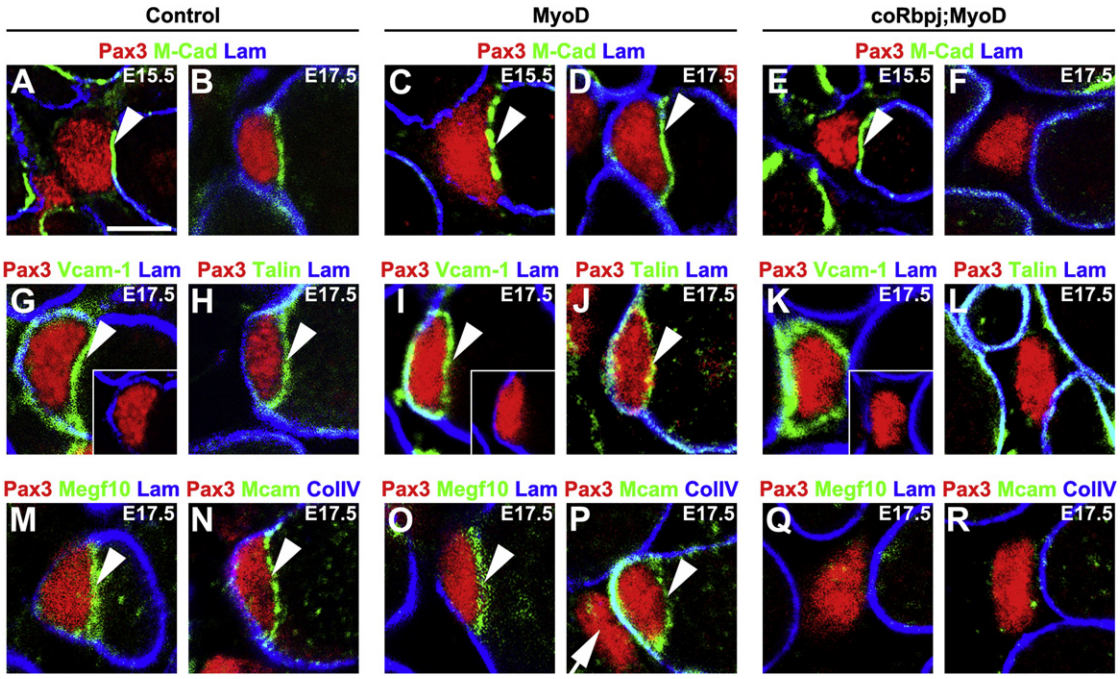

Figure 6. Notch Signals Control Adhesion of Emerging Satellite Cells

(A–L) Adhesive contacts between Pax3+ cells and myofibers in control (A, B, G, and H), *MyoD*$^{-/-}$ (C, D, I, and J), and *coRbpj;MyoD*$^{-/-}$ (E, F, K, and L) mice at indicated stages; the distribution of M-cadherin (A–F), Vcam-1 (G, I, and K), and talin (H, J, and L) was analyzed.

(M–R) Analysis of Megf10 (M, O, and Q) and Mcam (N, P, and R) distribution in the muscle of control (M and N), *MyoD*$^{-/-}$ (O and P), and *coRbpj;MyoD*$^{-/-}$ (Q and R) mice at indicated stages. Scale bar: 5 μm. See also Figure S6.

et al., 1996; Kuroda et al., 1999; Delfini et al., 2000; Hirsinger et al., 2001; Conboy and Rando, 2002; Schuster-Gossler et al., 2007; Vasyutina et al., 2007; Bjornson et al., 2012; Mourikis et al., 2012). Various mechanisms have been discussed to explain how Notch exerts this effect (for a recent review, see Buas and Kadesch, 2010). Our genetic analysis demonstrated that the drastic depletion of the pool of myogenic progenitor cells is rescued by a mutation of *MyoD*, indicating that a major role of Notch during fetal myogenesis is to repress *MyoD*. The Dll1 signal in the developing muscle appears to be provided by differentiating cells, i.e., myoblasts and myotubes (Hrabě de Angelis et al., 1997; Mourikis et al., 2012), indicating that Notch signaling adjusts the proportion of progenitors and differentiating cells, a mechanism that is similar to lateral inhibition during neurogenesis. MyoD and Myf5 act redundantly to control the entry into the myogenic differentiation program, and the presence of Myf5 can therefore account for the efficient myogenesis in *Notch/MyoD* double-mutant mice. However, Notch signals have additional important functions in late fetal myogenesis that go beyond *MyoD* suppression. In particular, satellite cell homing and assembly of a basal lamina around emerging satellite cells are severely disrupted in the rescued *Notch/MyoD* mutants.

Notch Signaling and the Satellite Cell Fate

The homing of emerging satellite cells is an important aspect of their biology. Here we propose that emerging satellite cells are driven into the interstitial space by a lack of Notch signals, and that such mislocated cells do not contribute to normal fiber growth in late fetal development. The aberrantly located myogenic progenitor cells observed in *Notch/MyoD* mutant mice are Pax3+ and thus are distinct from PW1+ cells, a recently identified interstitial cell population with myogenic potential that does not derive from the Pax3 lineage (Mitchell et al., 2010). *Pax7* is an important regulator of muscle stem cell physiology and is required for survival of satellite cells in the postnatal muscle (Seale et al., 2000; Oustanina et al., 2004). We find that Pax7 expression during development depends on Notch signals. Interestingly, others showed recently that Pax7 is upregulated in cultured satellite cells upon expression of the Notch intracellular domain (Wen et al., 2012). We conclude that canonical Notch signals suppress myogenic differentiation and contribute to important aspects of the satellite cell fate, such as Pax7 expression and homing.

We analyzed a series of mutants that affect canonical Notch signaling and observed a graded severity of the phenotypes. A depletion of muscle progenitor cells is observed in *coRbpj* and *Dll1*$^{LacZ/Ki}$ mutant mice at E17.5. In contrast, the expression of a dominant-negative variant of Maml1 results in a less severe but grave reduction of progenitor cells, indicating that the transcriptional responses to Notch signals are attenuated but not eliminated in this mutant. We show that an additional mutation of *MyoD* rescues the depletion of the progenitor pool irrespective of the nature of the Notch signaling mutation. Despite the rescue of the progenitor pool, further deficits became apparent in the late fetal period. Rbpj activates genes in a Notch-dependent manner (Kopan and Ilagan, 2009; Tanigaki and Honjo, 2010; Johnson and Macdonald, 2011), but we recently also observed a Notch-independent function of Rbpj in neuronal development

(Hori et al., 2008). The maintenance of myogenic progenitor cells via MyoD regulation, the strong effect on the homing of satellite cells, and Pax7 expression all depend on *Rbpj* and *Dll1*, and thus represent readouts of canonical Notch signaling.

Adhesion and Assembly of the Basal Lamina during Homing of Satellite Cells

Homing of satellite cells is a little-understood process that has not yet been analyzed on a molecular or cellular level. Our analyses show that this process is exquisitely regulated and that mutations can disrupt this process. Homing of satellite cells is basically abolished in *coRbpj;MyoD* mutant mice, accompanied by deficits in adhesion and basal lamina assembly. Our analyses indicate that Rbpj exerts cell-autonomous functions in muscle progenitor cells during homing. Instable adhesive interactions between myofibers and progenitor cells, and delayed assembly of the basal lamina provide a cellular basis for the colonization deficit. The assembly of a common basal lamina surrounding emerging satellite cells and the myofibers may stabilize the adhesive interactions in normal development, and sustained adhesion and basal lamina formation may thus be interdependent.

The single *MyoD* mutation results in the appearance of supernumerary myogenic cells that locate in the interstitial space. The presence of supernumerary myogenic cells in *MyoD* mutant mice was previously reported (Megeney et al., 1996), but it was not noted that these cells do not localize below the basal lamina of the myofiber. The lack of *MyoD* may preserve the progenitor status of interstitial cells by preventing their differentiation and instead result in their accumulation. Emerging satellite cells are heterogeneous, and approximately one-third of Pax3+/Pax7+ cells below the basal lamina in control mice coexpress MyoD (D.B., unpublished data). Lineage-tracing experiments have shown that a majority of adult satellite cells go through a MyoD+ state during development (Kanisicak et al., 2009), indicating that expression of *MyoD* is not always coupled to irreversible entry into the myogenic differentiation program. Thus, the *MyoD* mutation may exert cell-autonomous effects on a subpopulation of emerging satellite cells.

We identified a multitude of molecules that locate to adhesion sites between satellite cells and myofibers, including M-cadherin, Mcam, Megf10, and integrin $\alpha4\beta1$ and its corresponding counterreceptor, Vcam-1. Megf10 is an epidermal growth factor (EGF) repeat-containing transmembrane protein that is implicated in engulfment, adhesion, and myogenic differentiation (Holterman et al., 2007; Suzuki and Nakayama, 2007a, 2007b; Logan et al., 2011). Previous genetic analyses showed that integrin $\beta1$ serves major functions in myoblast fusion, precluding a genetic analysis during homing at a later stage in myogenesis (Cachaço et al., 2003; Schwander et al., 2003). Vcam-1 is not essential for adherence of satellite cells to myofibers, as assessed by analysis of conditional *Vcam1* mutation in mice ($Pax3^{cre};Vcam1^{flox/flox}$ mice; D.B., C.R., and C.B., unpublished data). M-cadherin plays a role in muscle regeneration but appears to have no major impact on muscle development (Hollnagel et al., 2002). Mutation of *MEGF10* in humans causes severe muscle deficits, and Megf10 impinges on Notch signaling in myogenesis (Holterman et al., 2007; Logan et al., 2011). We observed that *Odz4*, *Megf10*, and *Itga7* are downregulated in *Notch/MyoD* double-mutant muscle and that their expression directly responds to Notch signals. The various cell adhesion and basal lamina molecules identified here may act redundantly in timely, intricate ways to provide stable interactions when satellite cells emerge. Our work provides evidence that Notch signaling stimulates emerging satellite cells to contribute to the production of the basal lamina that will eventually surround both the satellite cell and the myofiber.

EXPERIMENTAL PROCEDURES

Mouse Strains

The $Rbpj^{flox}$, *MyoD*, *ROSA26-DnMaml*, $Dll1^{LacZ}$, $Dll1^{Ki}$, $Pax3^{cre}$, and *ROSA26-YFP* strains have been described previously (Rudnicki et al., 1992; Hrabě de Angelis et al., 1997; Srinivas et al., 2001; Han et al., 2002; Engleka et al., 2005; Tu et al., 2005; Schuster-Gossler et al., 2007). Unless otherwise indicated, we used heterozygous littermates, i.e., $MyoD^{+/-}$, *Rbpj* heterozygous ($Rbpj^{flox/+};Pax3^{cre}$), and double heterozygous ($Rbpj^{flox/+};MyoD^{+/-};Pax3^{cre}$) mice, for controls.

Isolation of Myogenic Progenitor Cells, Adult Satellite Cells, and Myofibers

Muscle tissue of E17.5 embryos or 3- to 4-week-old mice was dissected, treated with collagenase, and used for the isolation of single cells and for sorting. Single myofibers were isolated from the extensor carpi radialis longus and brachioradialis muscles of E15.5 and E19.5 embryos by a modification of a previously described protocol (Collins and Zammit, 2009). For more details, see Supplemental Experimental Procedures.

Immunohistochemistry and Electron Microscopy

Immunohistology was performed on cells fixed in 4% paraformaldehyde for 10 min, or on 12 μm cryosections of tissues fixed in 4% paraformaldehyde or Zamboni's fixative (paraformaldehyde/picric acid) for 2 hr. Electron microscopy on muscle was performed as described previously (Vasyutina et al., 2007). The antibodies used for immunohistological analyses are described in Supplemental Experimental Procedures.

qRT-PCR and Microarrays

Total RNA was isolated from FACS-isolated myogenic progenitor cells. PCR analysis after first-strand cDNA synthesis was performed using a CFX96 RT-PCR system (Bio-Rad, Hercules, CA). Microarray analysis was done using MouseRef-8 v2.0 Expression BeadChips (Illumina, San Diego, CA). Data were analyzed using GenomeStudio v2010.1 (Illumina) and the Partek Genomics Suite (Partek, St. Louis, MO). Genes that showed high differential expression in analysis of variance (Bonferroni-corrected, $p < 0.0001$) were selected. Microarray data have been deposited in the Gene Expression Omnibus (GEO) database under accession number GSE39379. See Supplemental Experimental Procedures for further details.

SUPPLEMENTAL INFORMATION

Supplemental Information includes six figures, one table, and Supplemental Experimental Procedures and can be found with this article online at http://dx.doi.org/10.1016/j.devcel.2012.07.014.

ACKNOWLEDGMENTS

We thank Tasuku Honjo (Kyoto University, Kyoto, Japan), Jonathan Epstein, Warren S. Pear (University of Pennsylvania, Philadelphia, PA), Achim Gossler (Universität Hannover, Germany), and Rudi Jaenisch (MIT, Cambridge, MA) for generously providing the $Rbpj^{flox}$, $Pax3^{cre}$, *DnMaml*, $Dll1^{lacZ/Ki}$, and *MyoD* mutant strains, respectively. We particularly thank Bettina Barby for technical assistance, Claudia Päseler, and Petra Stallerow for help with the animal husbandry and Walter Birchmeier and Alistair Garratt for critical discussions and for reading the manuscript. This work was funded by a grant from the Federal Ministry of Education and Research (SatNet) to C.B.

Received: December 2, 2011
Revised: June 19, 2012
Accepted: July 17, 2012
Published online: August 30, 2012

REFERENCES

Abou-Khalil, R., and Brack, A.S. (2010). Muscle stem cells and reversible quiescence: the role of sprouty. Cell Cycle *9*, 2575–2580.

Artavanis-Tsakonas, S., Rand, M.D., and Lake, R.J. (1999). Notch signaling: cell fate control and signal integration in development. Science *284*, 770–776.

Beatus, P., Lundkvist, J., Oberg, C., and Lendahl, U. (1999). The notch 3 intracellular domain represses notch 1-mediated activation through Hairy/Enhancer of split (HES) promoters. Development *126*, 3925–3935.

Bjornson, C.R., Cheung, T.H., Liu, L., Tripathi, P.V., Steeper, K.M., and Rando, T.A. (2012). Notch signaling is necessary to maintain quiescence in adult muscle stem cells. Stem Cells *30*, 232–242.

Buas, M.F., and Kadesch, T. (2010). Regulation of skeletal myogenesis by Notch. Exp. Cell Res. *316*, 3028–3033.

Buas, M.F., Kabak, S., and Kadesch, T. (2009). Inhibition of myogenesis by Notch: evidence for multiple pathways. J. Cell. Physiol. *218*, 84–93.

Cachaço, A.S., Chuva de Sousa Lopes, S.M., Kuikman, I., Bajanca, F., Abe, K., Baudoin, C., Sonnenberg, A., Mummery, C.L., and Thorsteinsdóttir, S. (2003). Knock-in of integrin beta 1D affects primary but not secondary myogenesis in mice. Development *130*, 1659–1671.

Collins, C.A., and Zammit, P.S. (2009). Isolation and grafting of single muscle fibres. Methods Mol. Biol. *482*, 319–330.

Collins, C.A., Olsen, I., Zammit, P.S., Heslop, L., Petrie, A., Partridge, T.A., and Morgan, J.E. (2005). Stem cell function, self-renewal, and behavioral heterogeneity of cells from the adult muscle satellite cell niche. Cell *122*, 289–301.

Conboy, I.M., and Rando, T.A. (2002). The regulation of Notch signaling controls satellite cell activation and cell fate determination in postnatal myogenesis. Dev. Cell *3*, 397–409.

Delfini, M.C., Hirsinger, E., Pourquié, O., and Duprez, D. (2000). Delta 1-activated notch inhibits muscle differentiation without affecting Myf5 and Pax3 expression in chick limb myogenesis. Development *127*, 5213–5224.

Engleka, K.A., Gitler, A.D., Zhang, M., Zhou, D.D., High, F.A., and Epstein, J.A. (2005). Insertion of Cre into the Pax3 locus creates a new allele of Splotch and identifies unexpected Pax3 derivatives. Dev. Biol. *280*, 396–406.

Fukada, S., Yamaguchi, M., Kokubo, H., Ogawa, R., Uezumi, A., Yoneda, T., Matev, M.M., Motohashi, N., Ito, T., Zolkiewska, A., et al. (2011). Hesr1 and Hesr3 are essential to generate undifferentiated quiescent satellite cells and to maintain satellite cell numbers. Development *138*, 4609–4619.

Gros, J., Manceau, M., Thomé, V., and Marcelle, C. (2005). A common somitic origin for embryonic muscle progenitors and satellite cells. Nature *435*, 954–958.

Han, H., Tanigaki, K., Yamamoto, N., Kuroda, K., Yoshimoto, M., Nakahata, T., Ikuta, K., and Honjo, T. (2002). Inducible gene knockout of transcription factor recombination signal binding protein-J reveals its essential role in T versus B lineage decision. Int. Immunol. *14*, 637–645.

Hirsinger, E., Malapert, P., Dubrulle, J., Delfini, M.C., Duprez, D., Henrique, D., Ish-Horowicz, D., and Pourquié, O. (2001). Notch signalling acts in postmitotic avian myogenic cells to control MyoD activation. Development *128*, 107–116.

Hollnagel, A., Grund, C., Franke, W.W., and Arnold, H.H. (2002). The cell adhesion molecule M-cadherin is not essential for muscle development and regeneration. Mol. Cell. Biol. *22*, 4760–4770.

Holterman, C.E., Le Grand, F., Kuang, S., Seale, P., and Rudnicki, M.A. (2007). Megf10 regulates the progression of the satellite cell myogenic program. J. Cell Biol. *179*, 911–922.

Hori, K., Cholewa-Waclaw, J., Nakada, Y., Glasgow, S.M., Masui, T., Henke, R.M., Wildner, H., Martarelli, B., Beres, T.M., Epstein, J.A., et al. (2008). A nonclassical bHLH Rbpj transcription factor complex is required for specification of GABAergic neurons independent of Notch signaling. Genes Dev. *22*, 166–178.

Hrabě de Angelis, M., McIntyre, J., 2nd, and Gossler, A. (1997). Maintenance of somite borders in mice requires the Delta homologue Dll1. Nature *386*, 717–721.

Jarriault, S., Brou, C., Logeat, F., Schroeter, E.H., Kopan, R., and Israel, A. (1995). Signalling downstream of activated mammalian Notch. Nature *377*, 355–358.

Johnson, J.E., and Macdonald, R.J. (2011). Notch-independent functions of CSL. Curr. Top. Dev. Biol. *97*, 55–74.

Kablar, B., Krastel, K., Tajbakhsh, S., and Rudnicki, M.A. (2003). Myf5 and MyoD activation define independent myogenic compartments during embryonic development. Dev. Biol. *258*, 307–318.

Kanisicak, O., Mendez, J.J., Yamamoto, S., Yamamoto, M., and Goldhamer, D.J. (2009). Progenitors of skeletal muscle satellite cells express the muscle determination gene, MyoD. Dev. Biol. *332*, 131–141.

Kassar-Duchossoy, L., Gayraud-Morel, B., Gomès, D., Rocancourt, D., Buckingham, M., Shinin, V., and Tajbakhsh, S. (2004). Mrf4 determines skeletal muscle identity in Myf5:Myod double-mutant mice. Nature *431*, 466–471.

Kassar-Duchossoy, L., Giacone, E., Gayraud-Morel, B., Jory, A., Gomès, D., and Tajbakhsh, S. (2005). Pax3/Pax7 mark a novel population of primitive myogenic cells during development. Genes Dev. *19*, 1426–1431.

Kimble, J., and Simpson, P. (1997). The LIN-12/Notch signaling pathway and its regulation. Annu. Rev. Cell Dev. Biol. *13*, 333–361.

Kitamoto, T., and Hanaoka, K. (2010). Notch3 null mutation in mice causes muscle hyperplasia by repetitive muscle regeneration. Stem Cells *28*, 2205–2216.

Kopan, R., and Ilagan, M.X. (2009). The canonical Notch signaling pathway: unfolding the activation mechanism. Cell *137*, 216–233.

Kopan, R., Nye, J.S., and Weintraub, H. (1994). The intracellular domain of mouse Notch: a constitutively activated repressor of myogenesis directed at the basic helix-loop-helix region of MyoD. Development *120*, 2385–2396.

Kuang, S., Kuroda, K., Le Grand, F., and Rudnicki, M.A. (2007). Asymmetric self-renewal and commitment of satellite stem cells in muscle. Cell *129*, 999–1010.

Kuang, S., Gillespie, M.A., and Rudnicki, M.A. (2008). Niche regulation of muscle satellite cell self-renewal and differentiation. Cell Stem Cell *2*, 22–31.

Kuroda, K., Tani, S., Tamura, K., Minoguchi, S., Kurooka, H., and Honjo, T. (1999). Delta-induced Notch signaling mediated by RBP-J inhibits MyoD expression and myogenesis. J. Biol. Chem. *274*, 7238–7244.

Lewis, J. (1998). Notch signalling and the control of cell fate choices in vertebrates. Semin. Cell Dev. Biol. *9*, 583–589.

Logan, C.V., Lucke, B., Pottinger, C., Abdelhamed, Z.A., Parry, D.A., Szymanska, K., Diggle, C.P., van Riesen, A., Morgan, J.E., Markham, G., et al. (2011). Mutations in MEGF10, a regulator of satellite cell myogenesis, cause early onset myopathy, areflexia, respiratory distress and dysphagia (EMARDD). Nat. Genet. *43*, 1189–1192.

Marneros, A.G., and Olsen, B.R. (2005). Physiological role of collagen XVIII and endostatin. FASEB J. *19*, 716–728.

Marthiens, V., Kazanis, I., Moss, L., Long, K., and Ffrench-Constant, C. (2010). Adhesion molecules in the stem cell niche—more than just staying in shape? J. Cell Sci. *123*, 1613–1622.

Mauro, A. (1961). Satellite cell of skeletal muscle fibers. J. Biophys. Biochem. Cytol. *9*, 493–495.

Mayer, U., Saher, G., Fässler, R., Bornemann, A., Echtermeyer, F., von der Mark, H., Miosge, N., Pöschl, E., and von der Mark, K. (1997). Absence of integrin alpha 7 causes a novel form of muscular dystrophy. Nat. Genet. *17*, 318–323.

Megeney, L.A., Kablar, B., Garrett, K., Anderson, J.E., and Rudnicki, M.A. (1996). MyoD is required for myogenic stem cell function in adult skeletal muscle. Genes Dev. *10*, 1173–1183.

Mitchell, K.J., Pannérec, A., Cadot, B., Parlakian, A., Besson, V., Gomes, E.R., Marazzi, G., and Sassoon, D.A. (2010). Identification and characterization of a non-satellite cell muscle resident progenitor during postnatal development. Nat. Cell Biol. *12*, 257–266.

Moser, M., Legate, K.R., Zent, R., and Fässler, R. (2009). The tail of integrins, talin, and kindlins. Science *324*, 895–899.

Mourikis, P., Sambasivan, R., Castel, D., Rocheteau, P., Bizzarro, V., and Tajbakhsh, S. (2012). A critical requirement for notch signaling in maintenance of the quiescent skeletal muscle stem cell state. Stem Cells *30*, 243–252.

Ouhtit, A., Gaur, R.L., Abd Elmageed, Z.Y., Fernando, A., Thouta, R., Trappey, A.K., Abdraboh, M.E., El-Sayyad, H.I., Rao, P., and Raj, M.G. (2009). Towards understanding the mode of action of the multifaceted cell adhesion receptor CD146. Biochim. Biophys. Acta *1795*, 130–136.

Oustanina, S., Hause, G., and Braun, T. (2004). Pax7 directs postnatal renewal and propagation of myogenic satellite cells but not their specification. EMBO J. *23*, 3430–3439.

Raymond, K., Deugnier, M.A., Faraldo, M.M., and Glukhova, M.A. (2009). Adhesion within the stem cell niches. Curr. Opin. Cell Biol. *21*, 623–629.

Relaix, F., and Marcelle, C. (2009). Muscle stem cells. Curr. Opin. Cell Biol. *21*, 748–753.

Relaix, F., Rocancourt, D., Mansouri, A., and Buckingham, M. (2005). A Pax3/Pax7-dependent population of skeletal muscle progenitor cells. Nature *435*, 948–953.

Rosen, G.D., Sanes, J.R., LaChance, R., Cunningham, J.M., Roman, J., and Dean, D.C. (1992). Roles for the integrin VLA-4 and its counter receptor VCAM-1 in myogenesis. Cell *69*, 1107–1119.

Rudnicki, M.A., Braun, T., Hinuma, S., and Jaenisch, R. (1992). Inactivation of MyoD in mice leads to up-regulation of the myogenic HLH gene Myf-5 and results in apparently normal muscle development. Cell *71*, 383–390.

Rudnicki, M.A., Schnegelsberg, P.N., Stead, R.H., Braun, T., Arnold, H.H., and Jaenisch, R. (1993). MyoD or Myf-5 is required for the formation of skeletal muscle. Cell *75*, 1351–1359.

Schuster-Gossler, K., Cordes, R., and Gossler, A. (2007). Premature myogenic differentiation and depletion of progenitor cells cause severe muscle hypotrophy in Delta1 mutants. Proc. Natl. Acad. Sci. USA *104*, 537–542.

Schwander, M., Leu, M., Stumm, M., Dorchies, O.M., Ruegg, U.T., Schittny, J., and Müller, U. (2003). Beta1 integrins regulate myoblast fusion and sarcomere assembly. Dev. Cell *4*, 673–685.

Seale, P., Sabourin, L.A., Girgis-Gabardo, A., Mansouri, A., Gruss, P., and Rudnicki, M.A. (2000). Pax7 is required for the specification of myogenic satellite cells. Cell *102*, 777–786.

Seale, P., Ishibashi, J., Holterman, C., and Rudnicki, M.A. (2004). Muscle satellite cell-specific genes identified by genetic profiling of MyoD-deficient myogenic cell. Dev. Biol. *275*, 287–300.

Shawber, C., Nofziger, D., Hsieh, J.J., Lindsell, C., Bögler, O., Hayward, D., and Weinmaster, G. (1996). Notch signaling inhibits muscle cell differentiation through a CBF1-independent pathway. Development *122*, 3765–3773.

Shea, K.L., Xiang, W., LaPorta, V.S., Licht, J.D., Keller, C., Basson, M.A., and Brack, A.S. (2010). Sprouty1 regulates reversible quiescence of a self-renewing adult muscle stem cell pool during regeneration. Cell Stem Cell *6*, 117–129.

Sherwood, R.I., Christensen, J.L., Conboy, I.M., Conboy, M.J., Rando, T.A., Weissman, I.L., and Wagers, A.J. (2004). Isolation of adult mouse myogenic progenitors: functional heterogeneity of cells within and engrafting skeletal muscle. Cell *119*, 543–554.

Song, X., Zhu, C.H., Doan, C., and Xie, T. (2002). Germline stem cells anchored by adherens junctions in the Drosophila ovary niches. Science *296*, 1855–1857.

Srinivas, S., Watanabe, T., Lin, C.S., William, C.M., Tanabe, Y., Jessell, T.M., and Costantini, F. (2001). Cre reporter strains produced by targeted insertion of EYFP and ECFP into the ROSA26 locus. BMC Dev. Biol. *1*, 4.

Suzuki, E., and Nakayama, M. (2007a). MEGF10 is a mammalian ortholog of CED-1 that interacts with clathrin assembly protein complex 2 medium chain and induces large vacuole formation. Exp. Cell Res. *313*, 3729–3742.

Suzuki, E., and Nakayama, M. (2007b). The mammalian Ced-1 ortholog MEGF10/KIAA1780 displays a novel adhesion pattern. Exp. Cell Res. *313*, 2451–2464.

Tanigaki, K., and Honjo, T. (2010). Two opposing roles of RBP-J in Notch signaling. Curr. Top. Dev. Biol. *92*, 231–252.

Tapscott, S.J. (2005). The circuitry of a master switch: Myod and the regulation of skeletal muscle gene transcription. Development *132*, 2685–2695.

Tu, L., Fang, T.C., Artis, D., Shestova, O., Pross, S.E., Maillard, I., and Pear, W.S. (2005). Notch signaling is an important regulator of type 2 immunity. J. Exp. Med. *202*, 1037–1042.

Vasyutina, E., Lenhard, D.C., Wende, H., Erdmann, B., Epstein, J.A., and Birchmeier, C. (2007). RBP-J (Rbpsuh) is essential to maintain muscle progenitor cells and to generate satellite cells. Proc. Natl. Acad. Sci. USA *104*, 4443–4448.

Wen, Y., Bi, P., Liu, W., Asakura, A., Keller, C., and Kuang, S. (2012). Constitutive Notch activation upregulates Pax7 and promotes the self-renewal of skeletal muscle satellite cells. Mol. Cell. Biol. *32*, 2300–2311.

White, R.B., Biérinx, A.S., Gnocchi, V.F., and Zammit, P.S. (2010). Dynamics of muscle fibre growth during postnatal mouse development. BMC Dev. Biol. *10*, 21.

Wu, L., Aster, J.C., Blacklow, S.C., Lake, R., Artavanis-Tsakonas, S., and Griffin, J.D. (2000). MAML1, a human homologue of Drosophila mastermind, is a transcriptional co-activator for NOTCH receptors. Nat. Genet. *26*, 484–489.